

## Quenching a rotating vortex in an excitable medium

V. Krinsky, F. Plaza, and V. Voignier

*Institut Non Linéaire de Nice, U.M.R 129 C.N.R.S. Université de Nice Sophia—Antipolis,  
1361, Rte. des Lucioles 06560 Valbonne, France*

(Received 5 December 1994)

We describe two mechanisms for the destruction of a rotating wave in an excitable medium by using (1) a wave containing no topological defects, and (2) a wave with a pair of topological defects of opposite charge. Both mechanisms result in the displacement of the core of the defect, and can be repeated as needed to expel the rotating wave out of the system. These two mechanisms provide a way of controlling initial stages of spatiotemporal chaos in excitable media. Applications to cardiac fibrillation are discussed.

PACS number(s): 05.45.+b, 05.70.Ln, 87.22.As, 87.10.+e

Spatiotemporal chaos in active media often takes the form of interacting topological defects, each of them corresponding to a rotating spiral wave. Defect mediated disorder was observed in Ginzburg-Landau equations [1], in the theoretical models of excitable media [2,3], in experiments in a chemical excitable medium [4], and in liquid crystals [5]. Approaches to control temporal [6] and spatiotemporal [7,8] chaos are based on the ideas of stabilizing unstable orbits. The approach proposed here to control spatiotemporal chaos in excitable media consists of destroying topological defects (note that transition to chaos in excitable media, e.g., in the cardiac muscle, can be initiated by nucleation of a single rotating wave only [9]).

The problem of quenching rotating waves has been intensively investigated in connection with cardiology, since rotating waves are responsible for the initiation of chaos in the cardiac muscle [10]. It was found in one-dimensional (1D) models [11] that an electrical impulse can stop wave rotation around a circle. Properly timed local electrical impulses are widely used in cardiology to restore normal wave propagation [11,12] and to prevent the transition to chaos. But this procedure [called anti-tachycardia pacing (ATP)] is not always efficient. The underlying mechanisms governing its success or failure are not yet clear. So, it is interesting to understand the underlying physics of the elimination of spiral waves.

A rotating wave is a robust structure, and only very special wave configurations, aimed at annihilating its topological charge, can be used. We describe here two mechanisms: First, quenching a vortex by means of a circular wave which (due to its zero topological charge) cannot directly annihilate with the initial vortex. However, its interaction with the vortex core results in the displacement of the latter over a distance of the order of the spiral wavelength. A vortex situated close to the boundary can thus be pushed out of the excitable medium and disappear. Second, quenching a vortex by using a pair of topological defects of opposite charges, one of them annihilating with the initial vortex, the other moving outside the medium.

Below we show a numerical simulation of the quenching of a rotating wave. The Barkley [13] model, a modification of van der Pol-type equations, which permits fast calculations, and catches the essential (topological) features of excitable media, was used:

$$\begin{aligned}\frac{\partial u}{\partial t} &= \varepsilon^{-1} u(1-u) [u - a^{-1}(v+b)] + \nabla^2 u, \\ \frac{\partial v}{\partial t} &= u - v.\end{aligned}\quad (1)$$

Here,  $u$  is an *activator* variable, describing the excitation, and  $v$  is an *inhibitor* variable; its slow dynamics are responsible for returning the system back to the resting point.

Mechanism 1 to quench the rotating spiral wave is shown in Fig. 1. A circular wave was used. When it reaches the core of the spiral, it induces its displacement [Fig. 1(f)]. This displacement quenches the spiral if its core or the wave tip are moved out of the medium [Fig. 1(f), dashed square].

Details of the wave interaction are shown in Figs. 1(a)–1(e). The circular wave was created by exciting the medium from an electrode [black square in Fig. 1(a)]. While propagating [Fig. 1(b)], the circular wave merges with the rotating wave [Fig. 1(c)]. Then the circular wave is broken [Fig. 1(d)] because propagation through the unrestored, or refractory wave tail [hatched in Fig. 1(d)] is impossible. The newly formed wave break 2 propagates along the refractory tail of the spiral [Figs. 1(d) and 1(e)]. Here it cannot curl into a rotating wave, because for this it should enter the refractory region. It curls up into a spiral wave only later [Fig. 1(f)], when it lags behind the rotating wave, and is not restricted anymore by its refractory tail. This results in a displacement of the core [Fig. 1(f)]. The displacement is an estimate of the efficiency of control of the rotating wave: the larger the displacement, the more efficient the method of control.

Mechanism 2 is shown in Fig. 2. A wave with a pair of topological defects of opposite charge [Fig. 2(b)] was

used. It was created by exciting the medium from the same electrode [black square in Figs. 1(a) and 2(a)]. Different results can be obtained depending on the state of the excitable medium at the electrode location. When a wave is rotating in the medium, the state of each point (situated outside the vortex core) changes periodically [Fig. 3(a)]. A circular wave is created when an electrode excites the medium which is sufficiently restored after the previous excitation [phase angle  $\theta > \theta_R$  in Fig. 3(a)]. No excitation can be induced when the medium is in the refractory state ( $\theta < \theta_L$ ), and a semicircular wave is created when the medium is in the intermediate, so called vulnerable state ( $\theta_L < \theta < \theta_R$ ) [14]. The vulnerable zone for the rotating spiral wave is shown as zone 3 in Fig. 3(b).

In Fig. 2(b), there are a total of three topological defects. If they evolve independently, they give rise to three rotating spiral waves. But when they are situated

close to one another, their interaction changes the result. The defects with opposite topological charges [defects 1 and 2 in Fig. 2(b)] fuse, wave tips interconnect, and the defects annihilate [Fig. 2(d)]. In the small box [dashed square in Fig. 2(d)], the remaining defect (3) is situated close to the boundary of the medium, merges with it, and disappears. The spiral wave is quenched. A version of this mechanism was described earlier [15].

In the general case, the defects are situated far from the boundary, and none of them merge with it. In this case, the rotating wave is not quenched, but appears located in another place [Fig. 2(e)].

The dependence of the shift of the rotating wave on the position of the electrode is shown in Fig. 4. Note a sharp jump in Fig. 4(C) at  $\theta \simeq 170^\circ$ ; here, mechanism 2 is replaced by mechanism 1. Note that mechanism 1 can be realized for a much larger range of phase angles  $\theta$  than mechanism 2; its effectiveness decreases with increasing

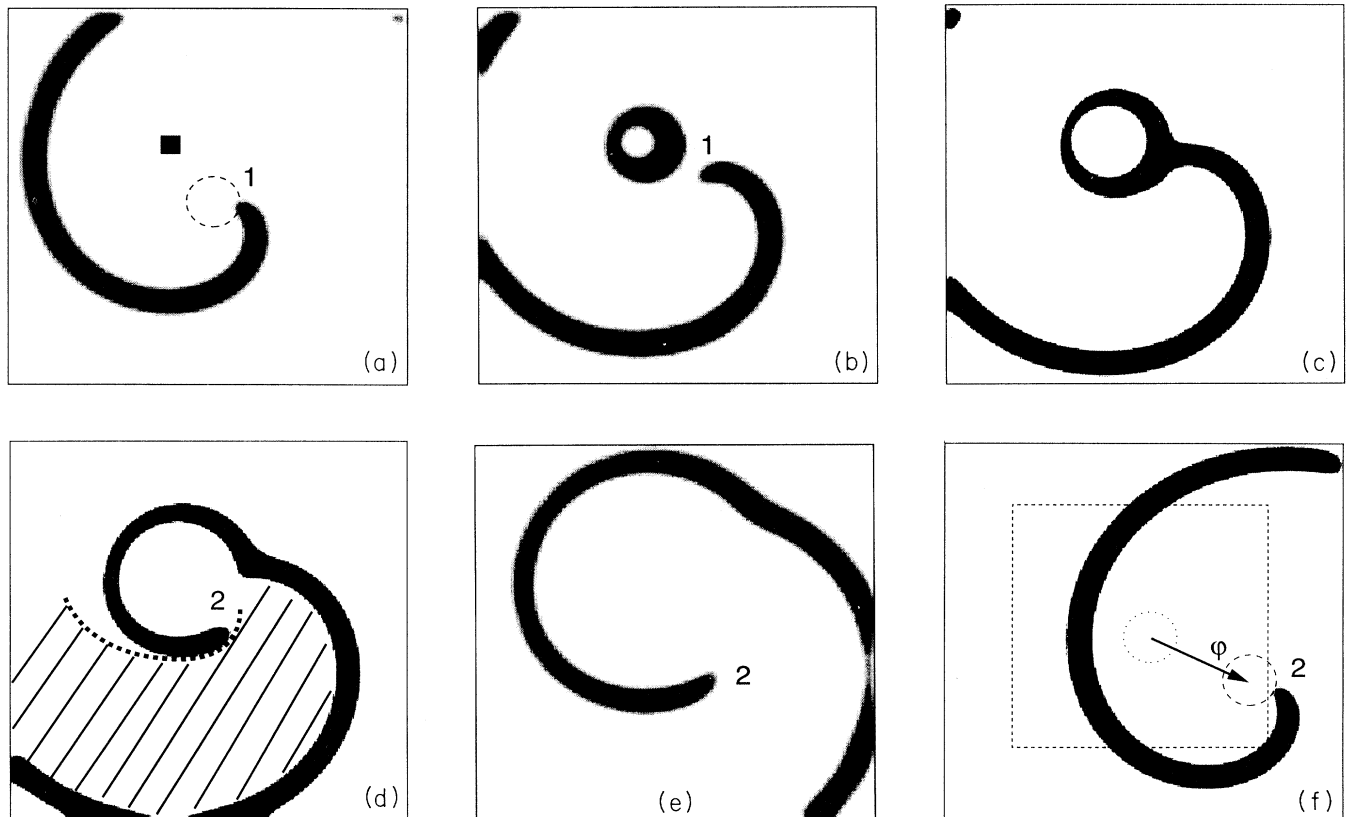


FIG. 1. The displacement and quenching of a spiral wave by a circular wave. (a)  $t = 0$ . Initial position of the spiral wave. The core is shown by a dashed line, the tip is labeled by 1. (b)  $t = 0.16$ . A circular wave created by a stimulus ( $u = 0.9$ ) delivered at  $t = 0$  from the electrode [black square in (a)]. (c)  $t = 0.25$ . The circular wave, while propagating, reaches the tip of the spiral wave. (d)  $t = 0.34$ . The circular wave is broken. The new tip is labeled by 2. The dashed line is the border of refractory tail (hatched). (e)  $t = 0.57$ . Tip 2 propagates along the refractory tail of initial spiral wave. (f)  $t = 2.15$ . In a box of smaller size ( $L = 17$ , dashed square), tip 3 has moved out of the medium, and the spiral wave is quenched. In the original box ( $L = 30$ ), tip 3 has formed a stationary rotating spiral wave. Its core is shown by dashed circle 2. The total displacement of the spiral wave is shown by the arrow. Two-dimensional numerical simulation of the Barkley model (grid:  $256 \times 256$  points,  $a = 0.53$ ,  $b = 0.05$ ,  $\varepsilon = 0.02$ ; size of the box  $L = 30$ ). Activator is visualized. The time unit is the period of rotation of the spiral.

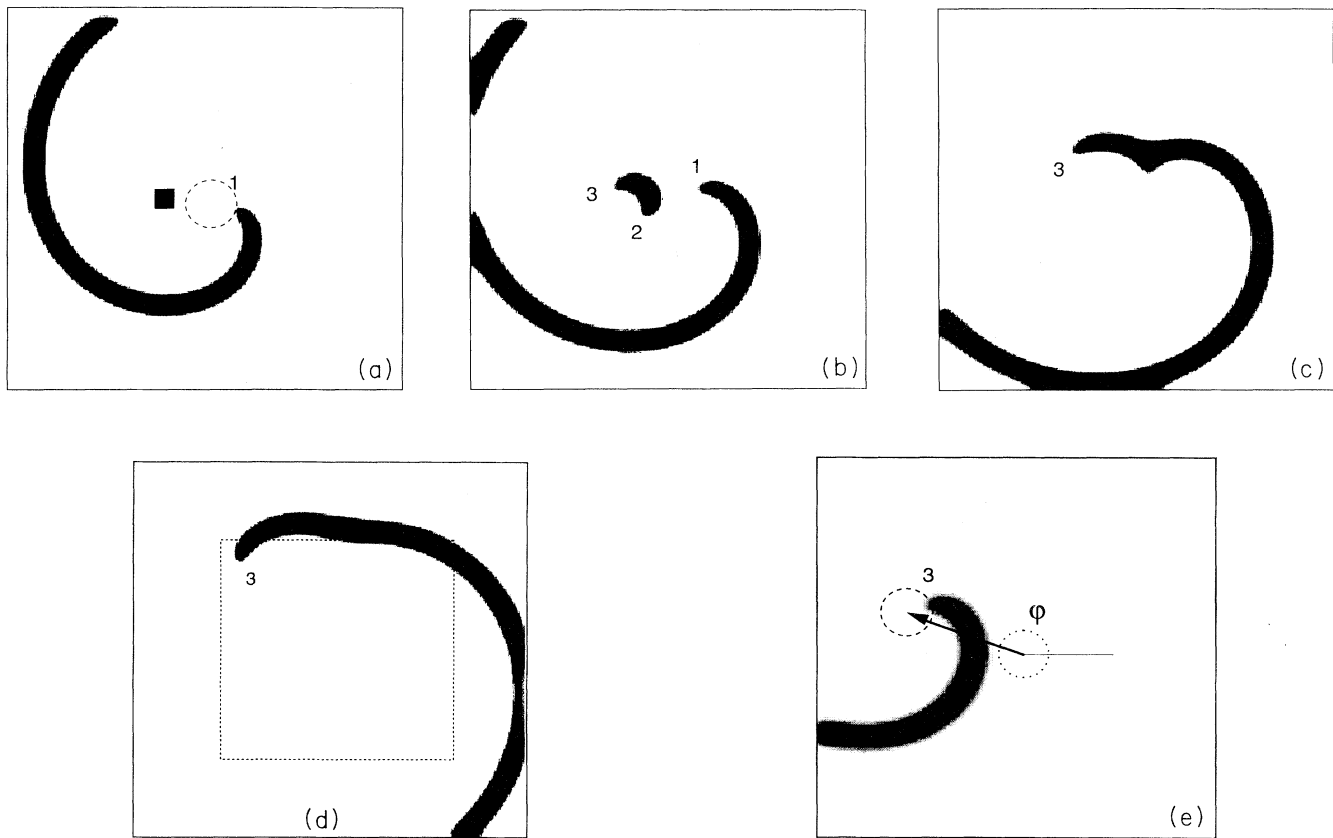


FIG. 2. The displacement and quenching of a spiral wave by a wave with two defects. (a)  $t = 0$ . Initial position of the spiral wave. The core is shown by a dashed line, the tip is marked by 1. (b)  $t = 0.13$ . A semicircular wave with two defects (tips 2 and 3) is created by a stimulus ( $u = 0.9$ ) delivered at  $t = 0$  from the electrode [black square in (a)]. (c)  $t = 0.3$ . The semicircular wave, while propagating, reaches the tip of the spiral wave. (d)  $t = 0.56$ . Tips 1 and 2 have annihilated. Again, there is only one defect (but it is situated at a new location). In a box of smaller size ( $L = 17$ , dashed square), tip 3 has reached the border, and the spiral wave is quenched. (e)  $t = 1.34$ . In the original box ( $L = 30$ ), tip 3 has formed a stationary rotating spiral wave. Its core is shown by dashed circle 3. The total displacement of the spiral wave is shown by an arrow. Parameters are the same as in Fig. 1.

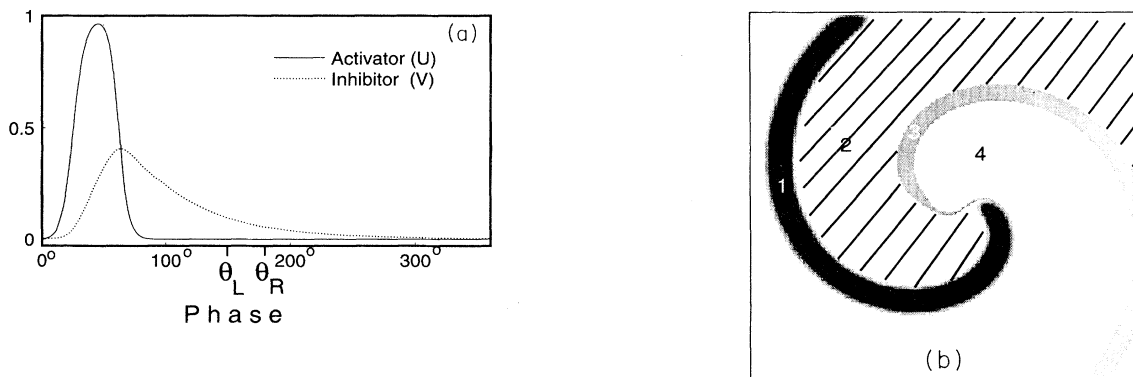


FIG. 3. (a) Distribution of activator and inhibitor in a rotating wave. (b) Space distribution of excitability. 1 is the excited zone, 2 is the refractory zone, 3 is the vulnerable zone, 4 is the resting zone. An electrical stimulus delivered in zone 4 creates a circular wave [as in Fig. 1(b)], in zone 3—a semicircular wave [a wave with two defects, as in Fig. 2(b)], in zones 1 or 2—does not create any wave.

$\theta$  [Fig. 4(B)] and with distance from the vortex core (not shown in the figure).

The mechanisms found here in a 2D excitable medium under the physics of eliminating rotating waves in cardiac muscle, and they are generic in the sense that they are not dependent upon the exact nature of excitable medium. Changing the model for the excitable medium

will affect the quantitative estimates only.

For both mechanisms, the shift of the rotating wave is about  $\lambda/2$  ( $\lambda$  is the spiral wavelength). In cardiac muscle,  $\lambda \simeq 10 - 20$  cm [10], so the results give a reasonable explanation for both the success and failure of the ATP technique used in cardiology for elimination of rotating waves. The appropriate geometry for modeling

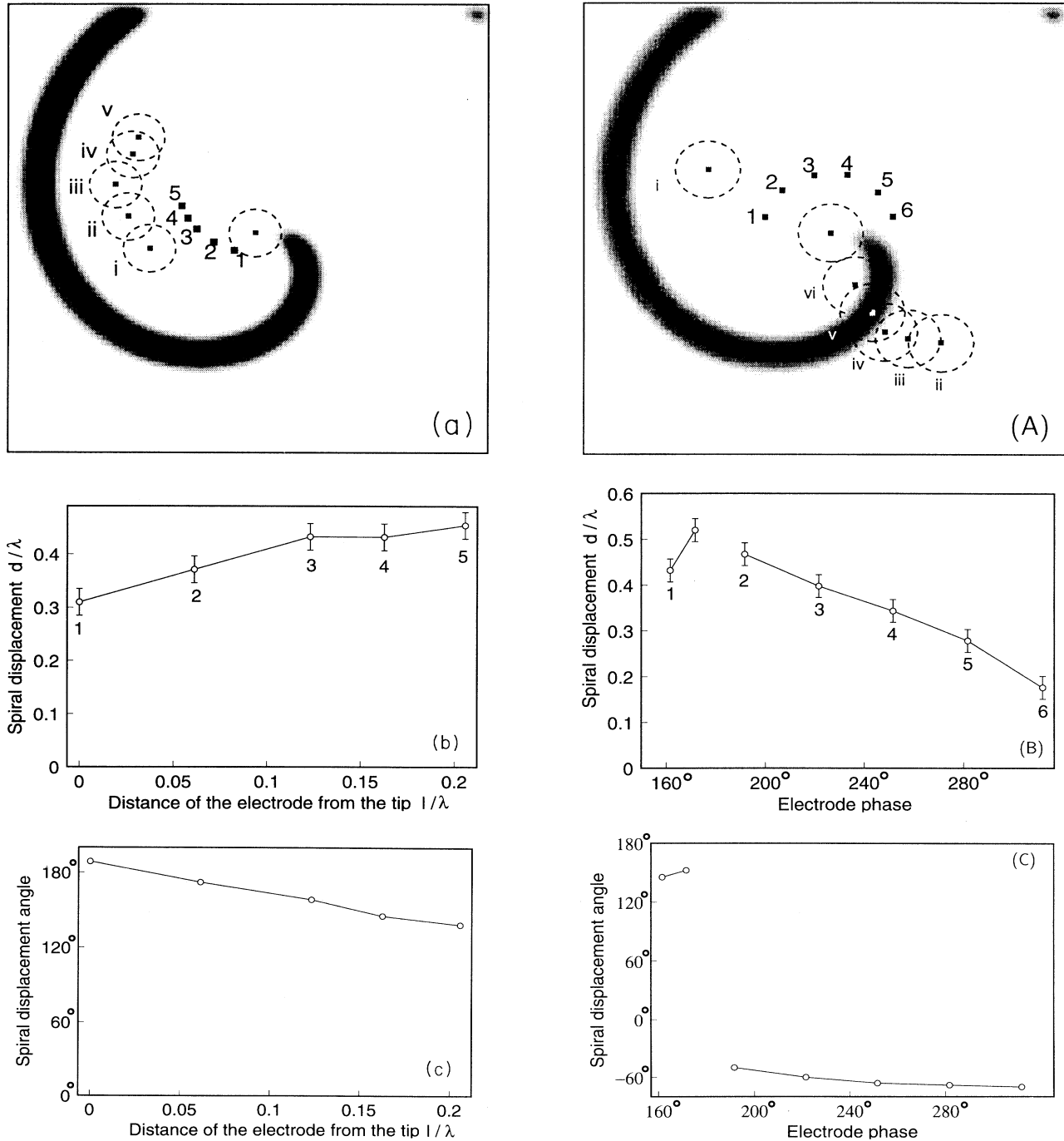


FIG. 4. Vortex displacement. Right column [(A)–(C)] displacement by a circular wave, left column [(a)–(c)]—by a wave with two defects. **a, A.** Electrode locations are shown by arabic numerals, new position of the vortex cores—by roman numerals. **b, B, c, C.** Dependence of the vortex displacement on parameters. The space unit is the wave length of the spiral.

excitation propagation in cardiac muscle is a semisphere with boundaries (because auricles are electrically insulated from ventricles). Its diameter is about 6 cm, so the distance to the boundaries is not larger than  $\lambda/2$ . But the real geometry is 3D. Of course, it is possible to move the spiral along the surface. But the spiral can also be moved perpendicular to the surface. Here, the spiral can be destroyed much more easily, because  $d \ll \lambda$  (thickness  $d$  of auricles is several mm).

It is interesting to notice the analogy between mechanism 1 and the phenomenon of wave induced drift [16]—a drift of a spiral induced by a wavetrain, with a frequency superior to the frequency of the spiral. The first few such waves annihilate with those emitted by the spiral; then as each new wave reaches the core of the spiral, the core-wave interaction creates a displacement of the spiral core.

Mechanism 2 looks like a high codimension phenomenon, as the exact reconnection of two vortices would

require the precise and unique location of the electrode. But this is not the case. First, the interaction between two closely spaced vortices helps their reconnection. This type of interaction has been studied in the Ginzburg-Landau equation, and gives qualitatively good prediction (two vortices of opposite charges attract, and annihilate when they are close enough, see, e.g., [17,18]). Second, in the case where the reconnection is not perfect, there remains a little “arm” to the wave, one small enough to shrink. In addition to vortex interactions, retraction mechanisms similar to the shrinking of a finger soliton (e.g., in liquid crystals) may be involved here. Further investigation of the underlying nonlinear wave problems may result in increasing the efficiency and creating new approaches to controlling rotating waves.

We are indebted to Jocelyne Lega for valuable discussions.

- 
- [1] P. Couillet, L. Gil, and J. Lega, *Phys. Rev. Lett.* **62**, 1619 (1989).
  - [2] E. Meron and P. Pelcé, *Phys. Rev. Lett.* **60**, 1880 (1988).
  - [3] A. Hadberg and E. Meron, *Phys. Rev. Lett.* **72**, 2494 (1994).
  - [4] K.I. Agladze, V.I. Krinsky, and A.M. Pertsov, *Nature* **308**, 834 (1984).
  - [5] T. Frisch and J. M. Gilli, *J. Phys. (France) II* **5**, 561 (1995).
  - [6] E. Ott, C. Grebogi, and J. A. Yorke, *Phys. Rev. Lett.* **64**, 1196 (1990).
  - [7] H. Gang and Q. Zhilin, *Phys. Rev. Lett.* **72**, 68 (1994).
  - [8] I. Aranson, H. Levine, and L. Tsimring, *Phys. Rev. Lett.* **72**, 2561 (1994).
  - [9] A. Karma, *Phys. Rev. Lett.* **71**, 1103 (1993).
  - [10] J. Davidenko *et al.*, *Nature* **355**, 349 (1992).
  - [11] J. Camm and D. Ward, *Pacing for Tachycardia Control* (Telectronics, London, 1983).
  - [12] J. Abildskov and R. Lux, *J. Electrocardiology* **27**, 277 (1994).
  - [13] D. Barkley, *Physica D* **49**, 61 (1991).
  - [14] C. F. Starmer, V. I. Krinsky, D. N. Romashko, and R. R. Aliev, in *Spatio-Temporal Organization in Nonequilibrium Systems*, edited by S. Mueller and Th. Plesser (Project Verlag, Dortmund, 1992), pp. 254–256.
  - [15] V.I. Krinsky, V.N. Biktashev, and A.M. Pertsov, *Ann. N.Y. Acad. Sci.* **591**, 232 (1990).
  - [16] V.I. Krinsky and K.I. Agladze, *Physica D* **8**, 50 (1983).
  - [17] S. Rica and E. Tirapegui, *Phys. Rev. Lett.* **64**, 878 (1990).
  - [18] I. S. Aranson, L. Kramer, and A. Weber, *Phys. Rev. E* **47**, 3123 (1993).

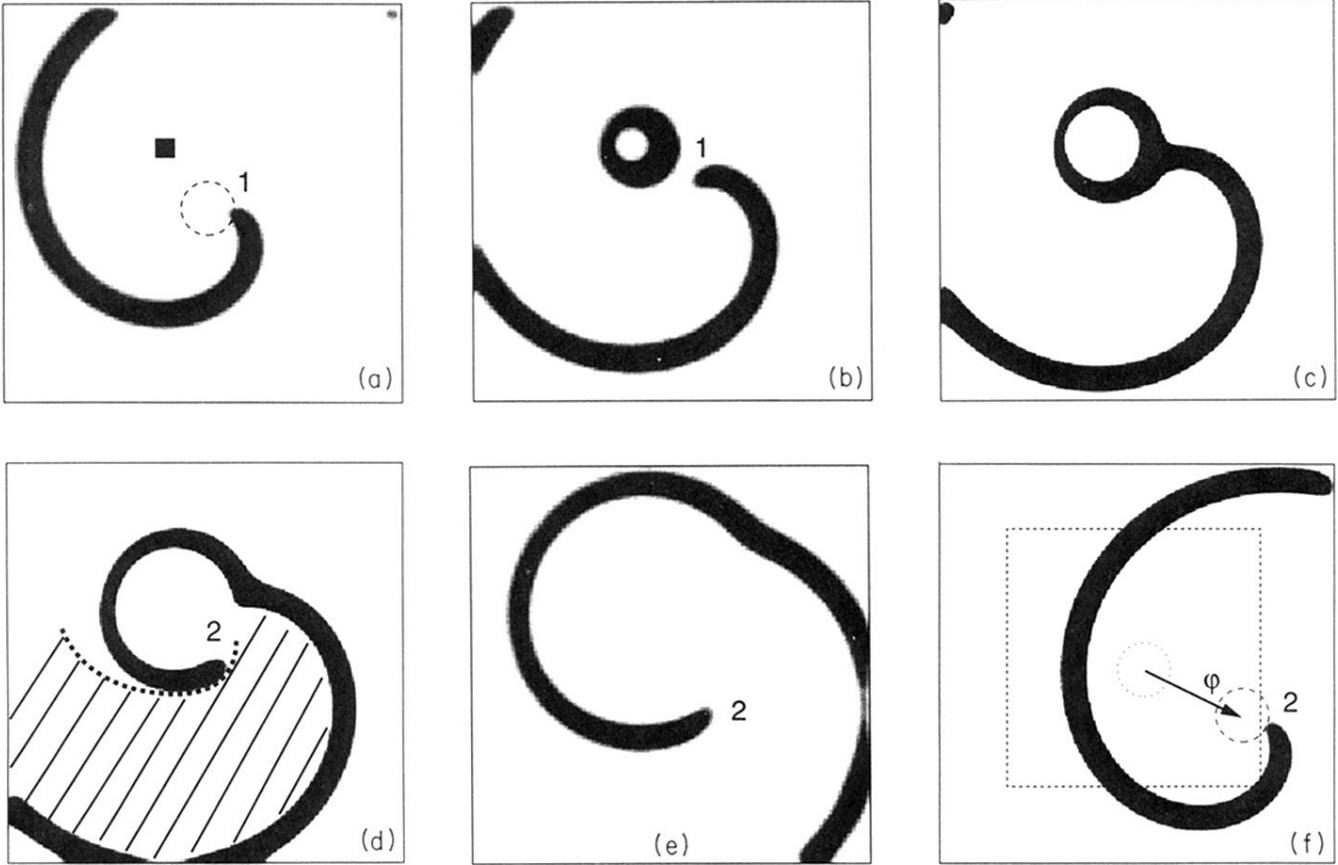


FIG. 1. The displacement and quenching of a spiral wave by a circular wave. (a)  $t = 0$ . Initial position of the spiral wave. The core is shown by a dashed line, the tip is labeled by 1. (b)  $t = 0.16$ . A circular wave created by a stimulus ( $u = 0.9$ ) delivered at  $t = 0$  from the electrode [black square in (a)]. (c)  $t = 0.25$ . The circular wave, while propagating, reaches the tip of the spiral wave. (d)  $t = 0.34$ . The circular wave is broken. The new tip is labeled by 2. The dashed line is the border of refractory tail (hatched). (e)  $t = 0.57$ . Tip 2 propagates along the refractory tail of initial spiral wave. (f)  $t = 2.15$ . In a box of smaller size ( $L = 17$ , dashed square), tip 3 has moved out of the medium, and the spiral wave is quenched. In the original box ( $L = 30$ ), tip 3 has formed a stationary rotating spiral wave. Its core is shown by dashed circle 2. The total displacement of the spiral wave is shown by the arrow. Two-dimensional numerical simulation of the Barkley model (grid:  $256 \times 256$  points,  $a = 0.53$ ,  $b = 0.05$ ,  $\varepsilon = 0.02$ ; size of the box  $L = 30$ ). Activator is visualized. The time unit is the period of rotation of the spiral.

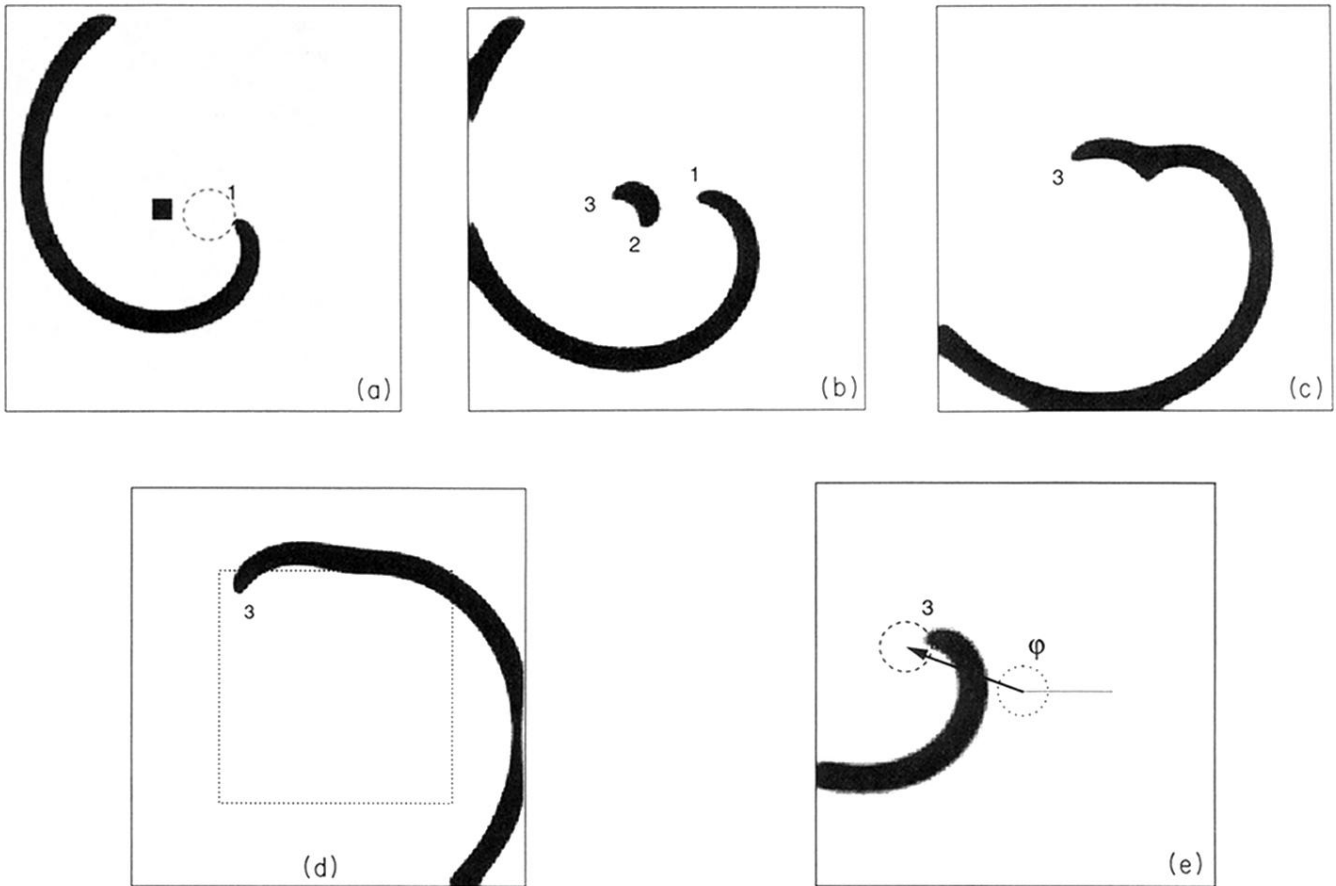


FIG. 2. The displacement and quenching of a spiral wave by a wave with two defects. (a)  $t = 0$ . Initial position of the spiral wave. The core is shown by a dashed line, the tip is marked by 1. (b)  $t = 0.13$ . A semicircular wave with two defects (tips 2 and 3) is created by a stimulus ( $u = 0.9$ ) delivered at  $t = 0$  from the electrode [black square in (a)]. (c)  $t = 0.3$ . The semicircular wave, while propagating, reaches the tip of the spiral wave. (d)  $t = 0.56$ . Tips 1 and 2 have annihilated. Again, there is only one defect (but it is situated at a new location). In a box of smaller size ( $L = 17$ , dashed square), tip 3 has reached the border, and the spiral wave is quenched. (e)  $t = 1.34$ . In the original box ( $L = 30$ ), tip 3 has formed a stationary rotating spiral wave. Its core is shown by dashed circle 3. The total displacement of the spiral wave is shown by an arrow. Parameters are the same as in Fig. 1.

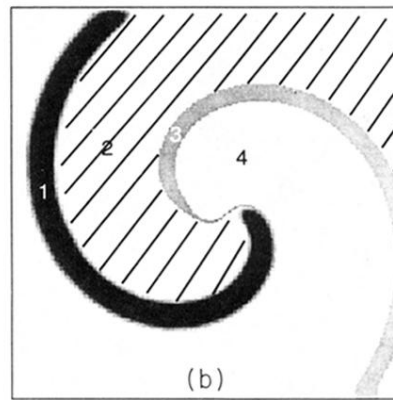
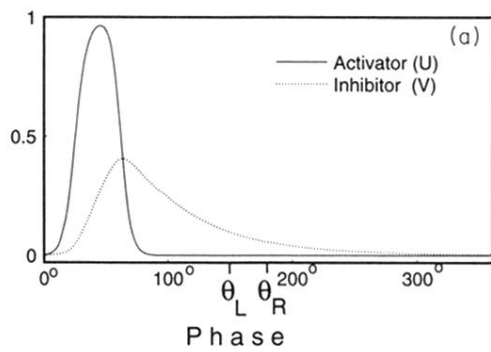


FIG. 3. (a) Distribution of activator and inhibitor in a rotating wave. (b) Space distribution of excitability. 1 is the excited zone, 2 is the refractory zone, 3 is the vulnerable zone, 4 is the resting zone. An electrical stimulus delivered in zone 4 creates a circular wave [as in Fig. 1(b)], in zone 3—a semicircular wave [a wave with two defects, as in Fig. 2(b)], in zones 1 or 2—does not create any wave.



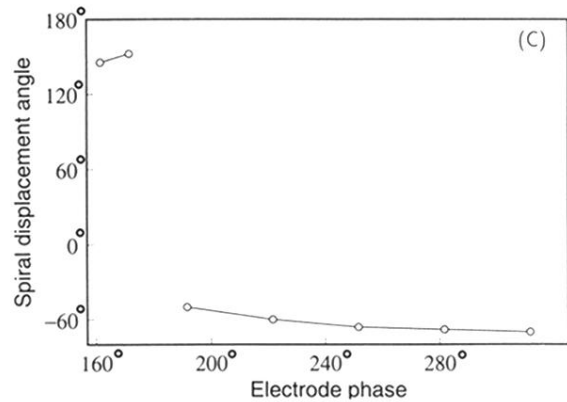
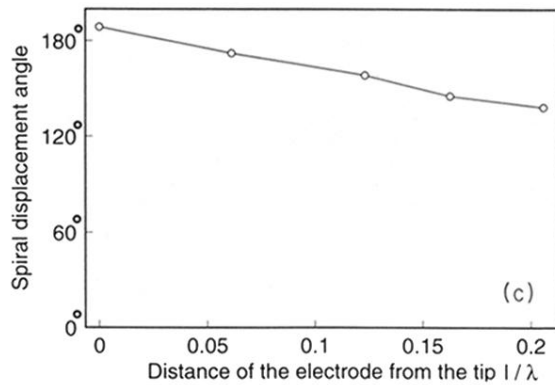
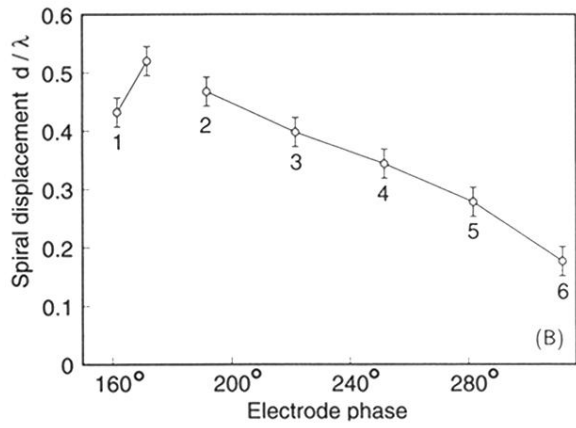
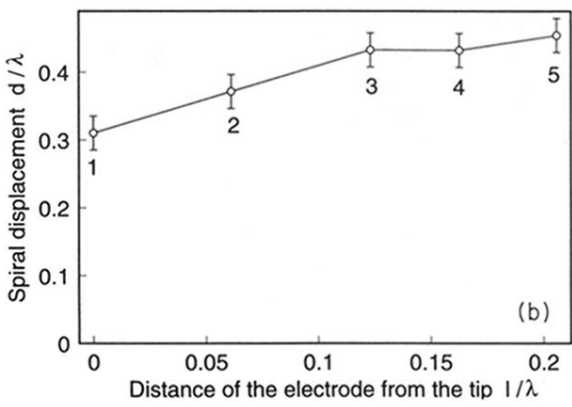
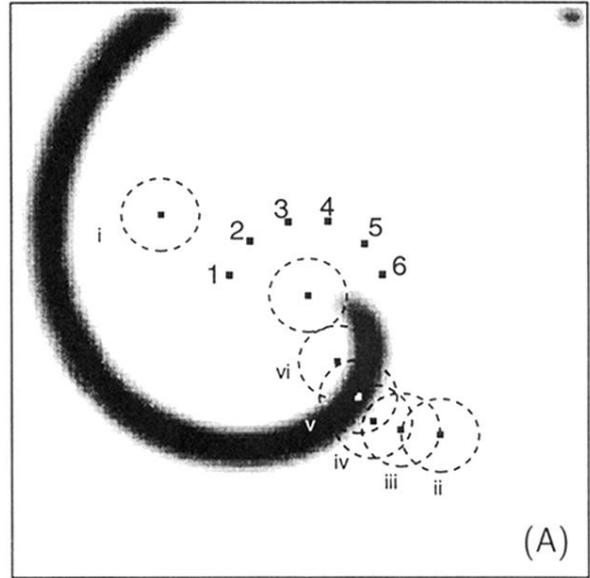
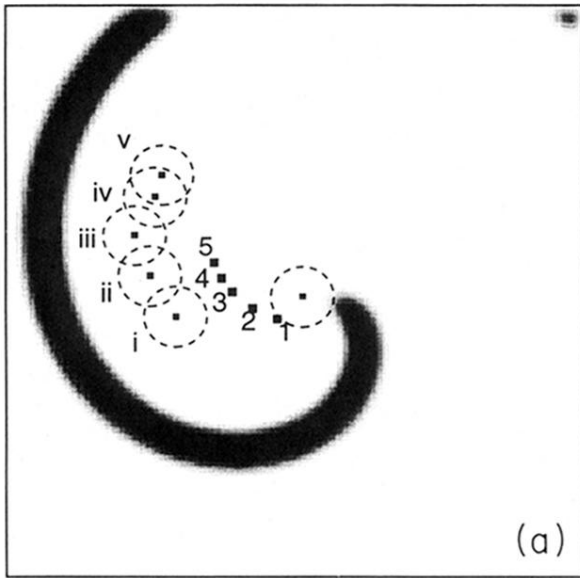


FIG. 4. Vortex displacement. Right column [(A)–(C)] displacement by a circular wave, left column [(a)–(c)]—by a wave with two defects. **a, A.** Electrode locations are shown by arabic numerals, new position of the vortex cores—by roman numerals. **b, B, c, C.** Dependence of the vortex displacement on parameters. The space unit is the wave length of the spiral.